Theor Chem Acc (2006) 116: 232–240
DOI 10.1007/s00214-005-0012-1

REGULAR ARTICLE

Fahmi Himo

Quantum chemical modeling of enzyme active sites and reaction mechanisms

Received: 3 August 2005 / Accepted: 11 August 2005 / Published online: 15 November 2005

Abstract Density functional methods, in particular the B3LYP functional, together with the explosive enhancement of computational power, have in the last 5 years or so made it possible to model enzyme active sites and reaction mechanisms in a quite realistic way. Many mechanistic problems have indeed been addressed and solved. This review gives a brief account of the methods and models used to study enzyme active sites and their reaction mechanisms using quantum chemical methods. Examples are given from our recent work in this field. Future perspectives of the field are discussed.

1 Introduction

With the development of Becke's B3LYP functional [1–4] in the early 1990s, quantum chemists were presented with a method that had an accuracy comparable with the most accurate ab initio methods but that is computationally much cheaper. Since then, B3LYP has been applied to a huge number of problems in diverse fields ranging from surface science to biochemistry.

Like other computational disciplines, quantum chemistry has benefited from the enormous increase in computer speed. As computers became faster and cheaper, increasingly larger systems could be treated. With the computer power of today, one is able to routinely handle systems of up to 100 atoms using the B3LYP functional with a medium size basis set.

Enzymes consist usually of many thousands of atoms. How can one then study the reactivity of enzymes using small quantum chemical clusters of say 80–100 atoms? It is not a priori obvious that this kind of model can work or at all provide information and understanding of the catalytic processes. One physical justification is that the energies involved in chemical reactions, bond breaking and formation, are usually much higher than long range electrostatics. The effect of the catalyst, in this case the active site of the enzyme, is thus to a large extent local, and environmental effects are usually of lower order. More importantly, the proof of the pudding is in the eating. The large number of investigations by many researchers in recent years testifies to the usefulness of such models.

The aim of this short review is to discuss strategies and experiences of how to use relatively small quantum chemical models to study enzyme active sites and reaction mechanisms using density functional methods. The various aspects of the models will be illustrated by examples from our recent work in this field. There exist some recent reviews that excellently cover different topics in other contexts [5–9]. This review will not discuss the use of QM/MM methods to study enzymatic reactions.

F. Himo
Theoretical Chemistry, Department of Biotechnology,
Royal Institute of Technology, Albanova University Center,
SE-106 91 Stockholm, Sweden
E-mail: himo@theochem.kth.se

2 Computational methods

The majority of quantum chemical studies of enzyme catalysis use the B3LYP functional [1–4], which is usually written as:

$$F^{\mathrm{B3LYP}} = A F_x^{\mathrm{HF}} + (1-A) F_x^{\mathrm{Slater}} + B F_x^{\mathrm{Becke}} + C F_c^{\mathrm{LYP}} + (1-C) F_c^{\mathrm{VWN}}$$

where F_x^{HF} is the Hartree–Fock exchange, F_x^{Slater} is the Slater exchange, F_x^{Becke} is the gradient part of the exchange functional of Becke, F_c^{LYP} is the correlation functional of Lee et al. [10] and F_c^{VWN} is the correlation functional of Vosko et al. [11]. The weighting coefficients A, B and C were determined by minimizing the average absolute deviation for the difference between theory and experiment for 116 atomic and molecular properties.

We will not discuss the accuracy of the B3LYP functional here, but suffice it to say that the available benchmark studies so far show two things. First, in terms of energies and geometries, the B3LYP functional is superior to the other current DFT functionals. Second, its accuracy is comparable to the most accurate ab initio methods [12–14]. Here, it is important to note that for other properties, like for instance magnetic and optical properties, this is not necessarily the case.

Usually, a relatively small basis set (typically of double zeta quality) is used for geometry optimizations. This gives, in general, quite reliable geometries that can then be used to obtain accurate energies using single point calculations with much larger basis sets (typically of triple zeta quality and including polarization and diffuse functions). When the size of the system permits, Hessians are calculated to confirm the nature of the stationary points and to evaluate zero-point vibrational effects.

3 Locating transition states

At the heart of the theoretical study of a catalytic process is the location and characterization of the transition state (TS). Once the TS is found and the energetic barrier is calculated, this can usually be related to experimental rates of reactions by means of the classical TS theory. The central assumption here is that the transition structure is in "pseudo" equilibrium with the reactants. This allows the derivation of the following basic formula

$$k = \frac{k_B T}{h} e^{-\Delta G/RT}$$

where ΔG is the difference in the Gibbs free energy between the TS and the reactants, T is the absolute temperature, R is the gas constant, k_B is the Boltzmann constant, and h is Planck's constant. This approximation works quite well for the purpose of substantiating or refuting reaction mechanisms, or to compare energies of different reaction pathways.

From TS theory, some useful rules of thumb can be derived. For example, at room temperature, a barrier of ca 18 kcal/mol corresponds to a rate constant of 1/s, and every increase (or decrease) of ca 1.4 kcal/mol in the barrier corresponds to a decrease (or increase) in rate by one order of magnitude. From this it is clear that the calculations cannot be used to calculate exact reaction rates, since an error of 3 kcal/mol in the activation barrier, which is tolerable in the calculations, corresponds to an error of two orders of magnitude in the rate.

Practically to be able to optimize TS structures, the starting geometry guess has to be quite good, typically in the quadratic region of the TS. A Hessian is also typically required to reach convergence. This Hessian calculation need not be at the same level of theory as the optimization. Many times it is sufficient to use Hartree–Fock Hessians with some small basis set. Lately we have managed to optimize a good number of quite complicated TS making use of a local Hessian approach. In this approach, numerical Hessian elements are calculated for only a few critical degrees of freedom and the rest of the matrix is estimated from low-level methods. This saves a lot of computational time and makes the TS optimization "cleaner" in many cases.

To obtain a good TS guess, there are some tricks to be used. A very useful one is to take advantage of the general experience that the local structure of a TS is to a large extent independent of the size of the model. Thus, we often perform the tedious work of finding the TS for as a small model as possible and then transfer the geometrical information (bond distances and angles) to the large model, which then makes it much easier to locate the TS. Note that although the local structure of the TS does not change much, the energies can differ a lot.

A recent study on the methyl transfer reaction in glycine N-methyltransferase (GNMT) serves as a good example here [15]. GNMT catalyzes the transfer of a methyl group from S-adenosylmethionine (SAM) to glycine, resulting in the formation of sarcosine (N-methylglycine) and S-adenosylhomocysteine (SAH) (Fig. 1a). The starting point for the calculations was a recent X-ray crystal structure of GNMT complexed with SAM and acetate [16]. We devised quantum chemical models of different sizes to study this S_N2 reaction [15]. The smallest model is composed of just glycine (neutral form) and an extremely truncated model of SAM, consisting of the sulfur center and one methyl on each side. In total, the size of this model is 23 atoms. As seen from the optimized TS structure shown in Fig. 1b, the critical S–C and C–N bond distances are 2.37 Å and 2.15 Å, respectively. This information was helpful when the full model (98 atoms) was used. Now, the SAM model is larger and several amino acids at the active site were included (see Fig. 1c). As seen, the local structure of the TS (in this case the S–C and C–N bond lengths) is quite close in the two models. While for the 23-atom model, the TS takes a couple of hours to find on a normal PC, one could spend much longer time searching for the TS of the large model if one starts from scratch. To go from small to larger models helps not only in speeding up the calculations but also in identifying and understanding the important factors contributing to the characteristics of the system.

Sometimes, a linear transit (LT) scan is used to obtain information about the barrier. In this scheme, one degree of freedom is chosen as a reaction coordinate and the value of this is kept fixed in steps while all other degrees of freedom are minimized. Provided that the reaction coordinate is well-chosen and the resulting energy curve is well-behaving (smooth curve), this procedure actually contains most of the necessary information to judge a reaction mechanism energetically. If, however, the chosen reaction coordinate does not represent the chemistry taking place, the calculations can suffer from hysteresis problems. These appear typically when several events happen at the same time, in a concerted reaction. When only one degree of freedom is stepped, one typically needs to push too far for changes to take place in the other degrees of freedom.

Let us illustrate this with some recent calculations on the reaction mechanism of deoxyribonucleotidase (dN) [17]. This Mg-dependent enzyme catalyzes the dephosphorylation of deoxyribonucleoside monophosphates to their nucleoside form in human cells (Fig. 2a). The first steps of the proposed reaction mechanism [17] of dN involve the coordination of the negatively charged phosphate part of the nucleotide (R-PO_4^{2-}) to the Mg^{2+} ion, upon which the Mg-ligand Asp41 performs a nucleophilic attack on the phosphorous atom of

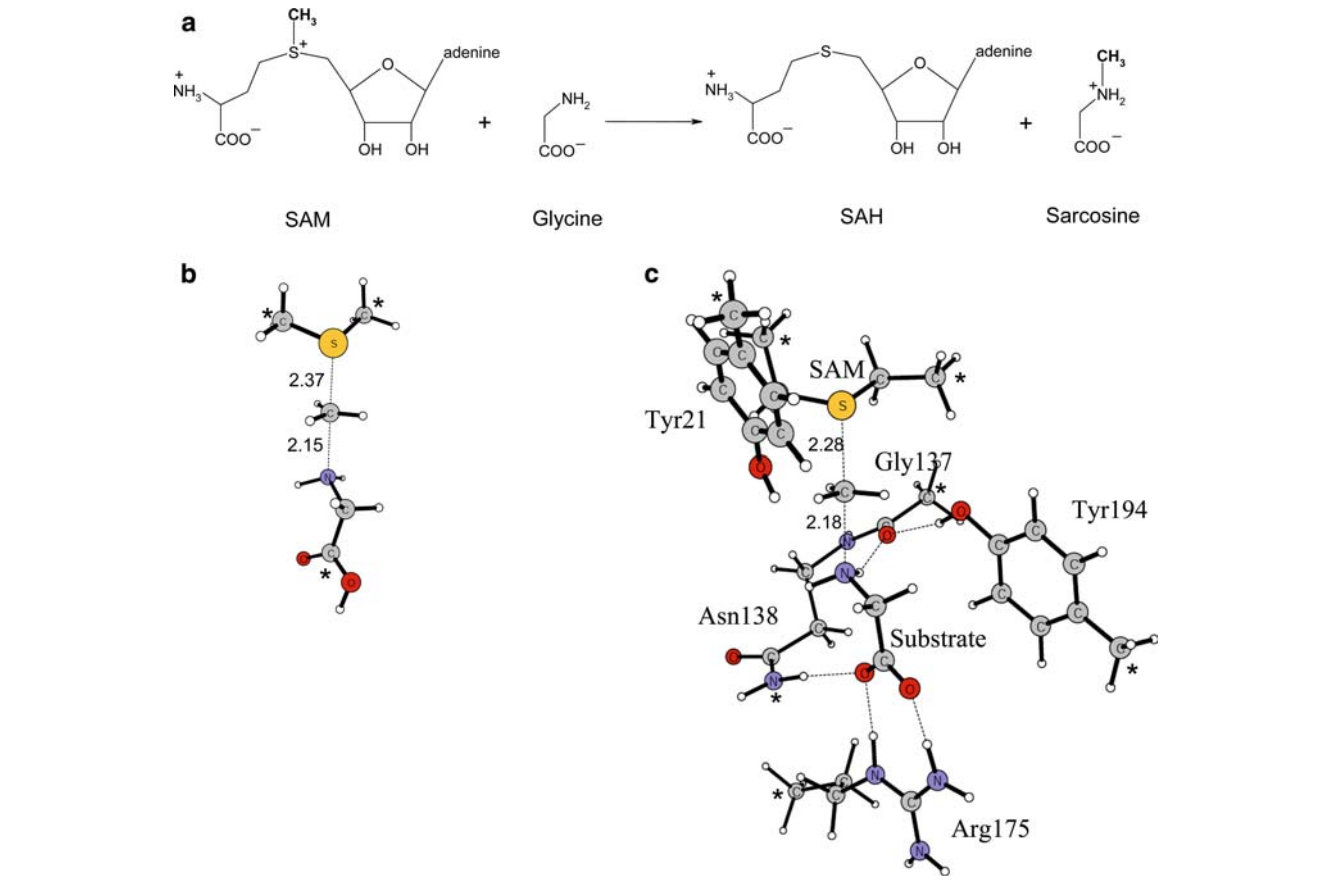

Fig. 1 **a** Reaction catalyzed by glycine N-methyl transferase (GNMT). **b** Optimized methyl transfer TS using a small model. **c** Optimized methyl transfer TS using a large model. Asterisks (*) show atoms kept frozen to their crystallographically observed positions in the calculations

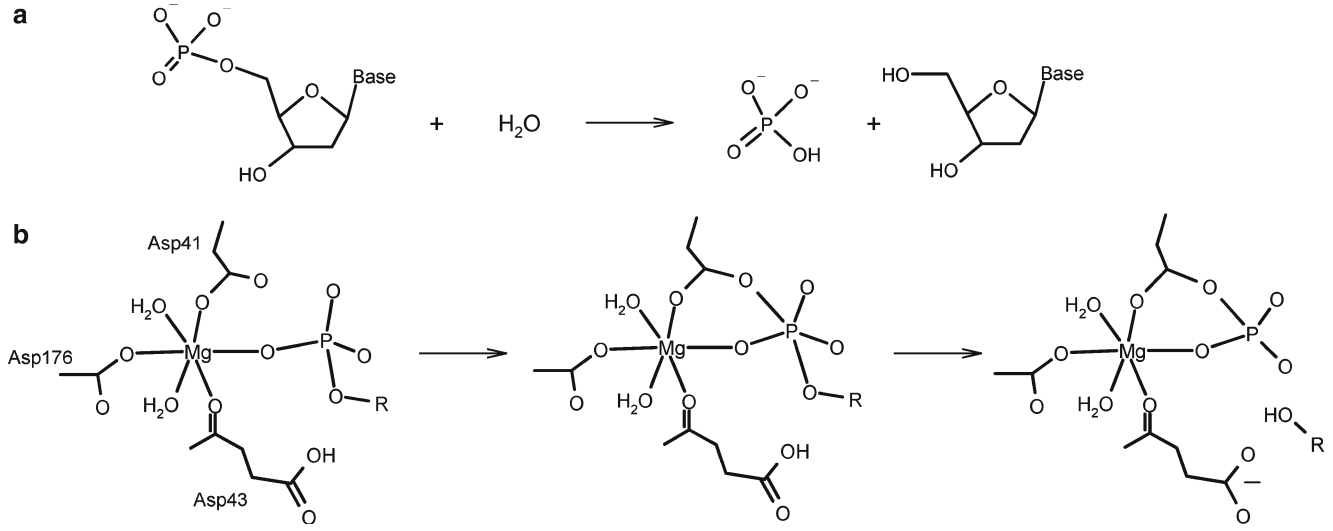

Fig. 2 **a** Reaction catalyzed by deoxyribonucleotidase (dN). **b** Proposed first steps in the mechanism of dN

the nucleotide with a subsequent formation of a hypothetical pentavalent phosphor–enzyme intermediate. In the next step, another Mg-ligand, Asp43 acts as an acid, protonating the leaving group (Fig. 2b).

Based on a recent X-ray crystal structure [17], a large quantum model was employed consisting of 99 atoms as shown in Fig. 3 (the details of the model will be discussed in next section). To study the nucleophilic attack step, we chose

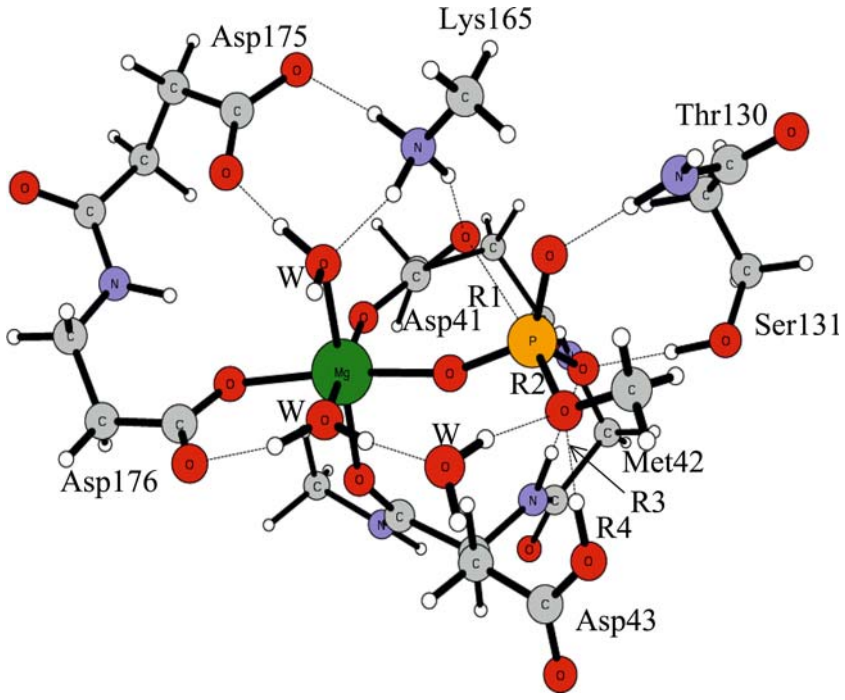

Fig. 3 Quantum chemical model used in the study of the dN reactions

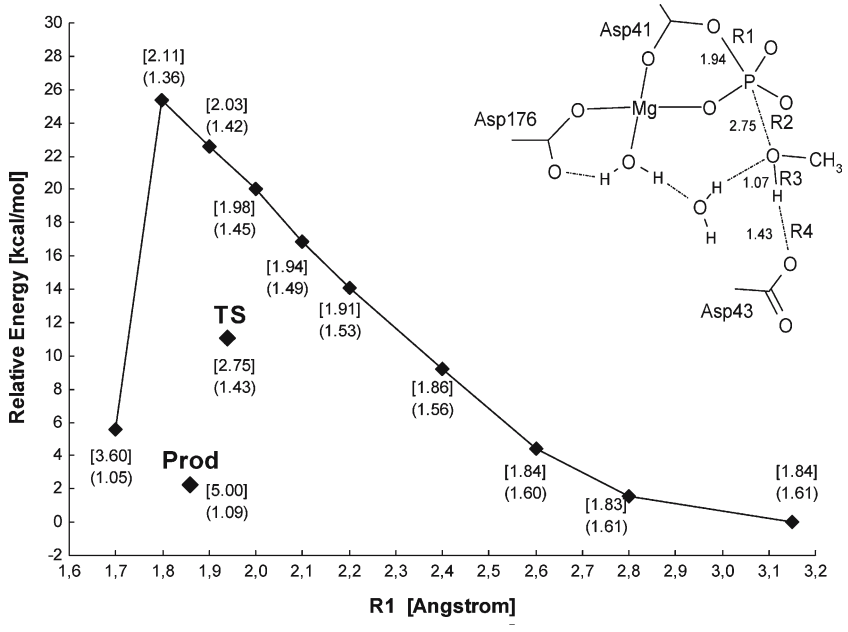

Fig. 4 Results of the linear transit calculations for dN. Isolated points represent the energies of the TS and product species. For each point, the values of R2 and R3 are given in Å in brackets and parentheses, respectively. *Insert* The distances obtained for the exact TS

the distance between O^{γ} of Asp41 and the P atom (called R1) as the reaction coordinate. R1 is fixed at different values and all other degrees of freedom are optimized in a LT scheme. The result of this procedure is shown in Fig. 4.

We see that as O^{γ} approaches P, i.e., R1 gets smaller, the *trans* P–O bond distance (called R2) increases slowly, and the carboxylic proton of Asp43 moves toward the leaving oxygen (R3 decreases and R4 increases). The energy increases until R1=1.8 Å, after which, a small change in R1 causes a big change in the energy. The proton of Asp43 now suddenly moves fully to the nucleoside, which then dissociates completely from the phosphate. The fully optimized product of this reaction step (with unconstrained R1) has an R1 value of 1.86 Å, i.e., larger than the R1=1.70 Å distance at which

the nucleoside dissociates. This is a clear sign of hysteresis problems.

The highest energy obtained using the LT scheme is found for R1=1.80 and is 25.4 kcal/mol. The sudden drop in energy after that point makes, of course, this energy unreliable. We have managed to optimize the exact unconstrained TS for this reactions step and the barrier is indeed considerably lower than the LT result, calculated to 11.1 kcal/mol. The R1 and R2 distances at the TS are 1.94 and 2.75 Å respectively, to be compared to the 1.80 and 2.11 Å obtained for the highest point of the LT. This example exposes some of the risks of using LT approach with a preassumed reaction coordinate.

4 Protein surrounding

The protein surrounding can affect the reactions in two major ways, namely by long-range polarization and by imposing steric restraints on the active site. In the quantum chemical approach used here, these effects are taken care of in different ways.

To account for the polarization effects caused by the part of the surrounding enzyme that is not explicitly included in the quantum model, cavity techniques can be used. This approximation assumes that the surrounding is a homogenous polarizable medium with some dielectric constant, usually chosen to be $\varepsilon = 4$ for protein environment.

Obviously, the further away we are from the active site, the better this approximation works, i.e., when a large model of the active site is used, most of the polarization effects are already explicitly included in the quantum calculations. This, in addition to the fact that the solvation effect saturates very quickly as a function of ε, makes the particular choice of the dielectric constant less critical. Typically, the relative solvation between minima and TS is calculated to be quite small, in the order of a few kilocalories/mol. In some cases, larger effects can be obtained, especially when charges are created or quenched close to the edge of the quantum model. When large solvent effects are obtained, it is usually an indication that some important parts are missing in the quantum model and need to be included. The solvation energies are usually calculated as single points on top of the gas-phase optimized geometries.

How well does this polarizable continuum model (PCM) approximation work? The answer turns on the question. If we are interested in finding out the smallest details about the energy contributions of the different parts of the enzyme, then this model is not sufficient. But if we are interested in finding the reaction pathway and compare the energies with competing reaction mechanisms, then the accuracy of the PCM calculations is usually sufficient.

One way to account for steric effects, at least approximately, is to use a freezing scheme. The enzyme environment can prevent a certain group from moving in a certain way or from making a certain rotation. Groups that are not bound to a metal center or linked by bonds or hydrogen bonds to some other groups at the active site move typically in shallow potential wells. In the small quantum chemical models, if not constrained somehow during the geometry optimizations, these groups can move a lot, even if the energetic driving force is very small. In order to keep the various groups in place to resemble the crystal structure as much as possible, certain atoms in the model, typically were the truncation is done, are kept frozen to their X-ray positions. This approach ensures structural integrity of the model, yet allows some flexibility of the various groups. Again, the error made by this approximation becomes smaller as the freezing points move further away from the active site, i.e., as the size of the quantum model increases.

The combination of continuum solvation and the freezing scheme represents in our opinion quite a good alternative to the demanding and cumbersome QM/MM calculations.

5 Active site models

Usually, to study reaction pathways and to find the intermediates and TS, a large number of calculations are required. It is hence extremely important to keep the size of the quantum chemical model as small as possible to answer questions. At the same time, it is crucial to choose the model such that the chemistry that takes place is accurately represented and no essential groups are left out.

As discussed above, the computational methods available today allow for accurate treatment of ca 100 atoms in reasonable time. Although this is a huge improvement compared to a few years ago, it is still very small, considering that an enzyme typically consists of thousands of atoms.

In a sense, every enzyme active site is unique and the quantum chemical model has to be considered individually. However, in the last few years, several guidelines on to how to model various situations have emerged. In this section, some typical cases and strategies will be discussed.

The models start typically from a crystal structure of the enzyme. This is, however, not an absolute requirement. Sometimes there exists enough biochemical and spectroscopic data to help construct a model and solve a particular problem. It ultimately depends on the questions posed.

5.1 Metal sites

In the case of metalloproteins, a large portion of the catalysis is dictated by the electronic structure of the metal ion and its immediate environment. A correct model of a metal active site should hence represent the electronic structure of the metal correctly. To achieve this, it is in many cases sufficient to include only the first coordination shell of the metal on top of which a PCM calculation is performed, to evaluate the solvation. In situations where some second shell residues are known from experiments, or can be suspected to influence the reactions, they are included explicitly. In instances where the metal site is particularly large, including several metal centers, some of the ligands that do not directly participate

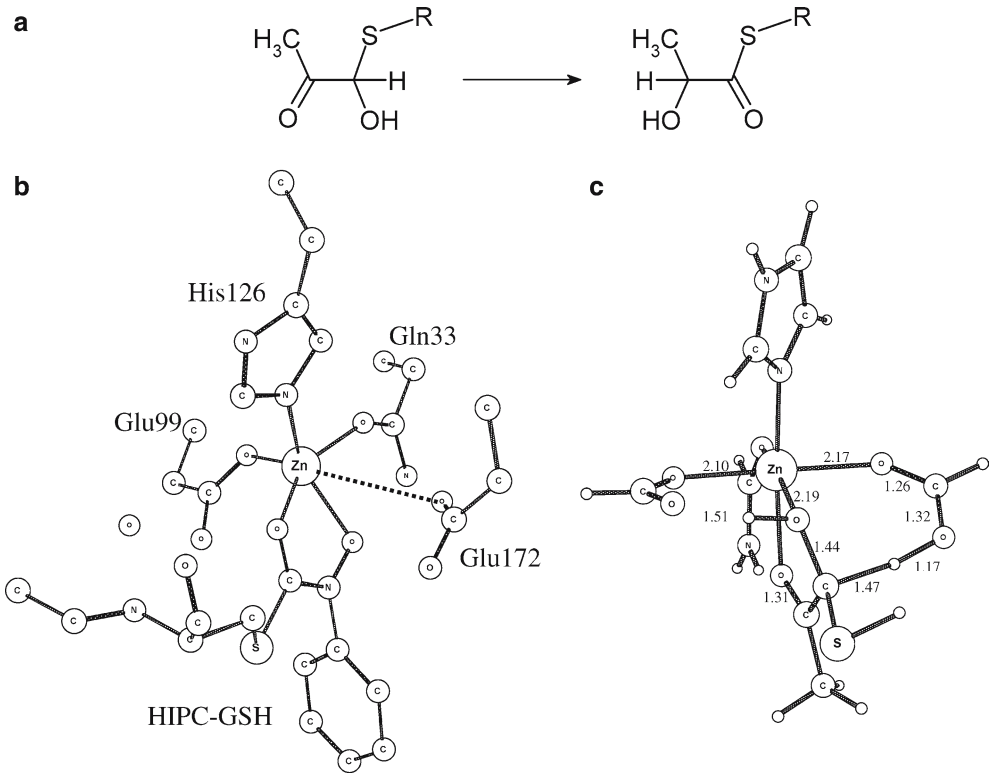

Fig. 5 **a** Reaction catalyzed by Glyoxalase I (GlxI). **b** X-ray crystal structure of the Zn site in complex with a TS analogue. **c** Optimized TS structure of the initial proton transfer step

in the chemistry can be replaced by simpler ligands, such as water or ammonia, as a first approximation. This approach was popular a few years ago, when one could not afford any better option, but has now almost completely disappeared.

To illustrate some of the points concerned with the modeling of metal active sites, let us start with a case where a relatively small model could help substantiating a proposed mechanism.

Glyoxalase I (GlxI) is a Zn-enzyme that converts hemithioacetal to S-D-lactoylglutathione, a reaction that involves shuttling of two protons (Fig. 5a). X-ray crystal structures showed that the Zn coordination consists of four protein residues (Gln33, Glu99, Glu172, His126) and two water molecules in an octahedral arrangement. Based on a structure with a TS analogue, the substrate is believed to bind bidentately to the Zn, replacing the two water molecules (Fig. 5b) [18]. The catalytic mechanism of GlxI was investigated using the B3LYP functional [19]. In the calculations, only the first shell ligands were included and they were modeled in the following way: the histidine using an imidazole, the glutamates using formates, and the glutamine using formamide. The hemithioacetal substrate was truncated at the sulfur of the glutathione (see Fig. 5c). The total size of the model is thus only 36 atoms. The surrounding protein was included using a PCM model, with ε=4. The first step in the catalytic mechanism of GlxI is proposed to be a proton transfer from substrate C1 to Glu172. Figure 5c shows the optimized TS structure for this reaction step.

The calculated barrier using this small model in conjunction with the PCM solvation is 14.4 kcal/mol, in excellent agreement with the known reaction rate ($k_{cat} \sim 1500\,s^{-1}$, corresponding to an activation barrier of ~14 kcal/mol). The critical C–H distance at the TS is 1.47 Å and the H–O distance is 1.17 Å. Based on the long Zn-Glu172 distance observed in the crystal structure (Fig. 5b), it was previously proposed that the Glu residue has to dissociate from the Zn ion in order to have a p K_a value close to that of the substrate, which is modified by the Zn-ligation [18]. From the QM results it could be concluded that Glu172 is perfectly capable of affecting the initial proton abstraction step without the need to displace it from the Zn. The Zn-ligation is evidently sufficient to reduce the pK_a of the substrate and make the proton transfer feasible.

It is interesting to note that the QM results are in excellent agreement with the results of Åqvist and co-workers, who used a combination of molecular dynamics simulations, free energy perturbation and empirical valence bond techniques to study the energetics of the same reaction step [20]. The Zn-catalyzed activation free energy was calculated to be ca 13 kcal/mol.

As seen, for GlxI, no second-shell residues were needed in the model. For the above-mentioned deoxyriboncleotidase case, on the other hand, a model consisting of 99 atoms and including several second-shell residues was needed, as displayed in Fig. 3 [17]. In this model, the following parts are included: the Mg^{2+} ion with its ligands Asp176, Asp41, Asp43, and two water molecules. Interestingly, Asp43 is coordinated

to the Mg by its carbonyl oxygen, and not its carboxylate, which will be involved in the proton transfer events. The backbone atoms of Met42 were included for two reasons. First, they form a bridge between the Mg ligands Asp41 and Asp43. Second, the peptide bonds of this residue form hydrogen bonds to the substrate oxygens and are thus needed to stabilize the negative charge of the substrate. For the same reason, parts of Thr130 and Ser131 were included. A model of the positively charged side chain of Lys165 was included, as it forms three hydrogen bonds to the different oxygens and hence contributes to the overall stability of the model. Asp175 was included in its entirety. The substrate was modeled using a $PO_4CH_3^{2-}$ moiety. This is adequate and resembles the properties of the P–O and H–O bond of the nucleotide quite well. Finally, an ordered water molecule that forms a hydrogen bond to the substrate was also included.

With all these parts, the total charge of this model becomes −2, and no atoms need to be frozen in order to get a good agreement with the crystal structure, which is a good indication that the model contains the essential parts needed. Interestingly, most of the residues included in this model correspond to residues that are conserved among the dNs.

5.2 Non-metal sites

In contrast to metalloproteins, where the metal ion helps keeping the different active site groups together, active sites of non-metal enzymes are typically formed like a pocket where the substrates dock. Usually, it is necessary to fix some centers to avoid very large movements of the residues.

In the GNMT study mentioned above [15], the model consisted of the following parts (see Fig. 1c): (a) A model of SAM, which is truncated two carbons away in each direction from the sulfur center. This is sufficient to model the properties of the S_D–C_E bond and to grant some flexibility to the SAM-model. (b) The glycine substrate, which was modeled based on the structure of the acetate, to which an amino group was added. (c) The side chain of Arg175. This group forms strong hydrogen bonds to the carboxylate of glycine and is hence essential to bind the substrate and stabilize its charge. (d) Parts of Gly137 and Asn138, as these groups are found to form hydrogen bonds to both the amino and the carboxylate groups of glycine substrate. (e) The phenol group of Tyr194, since this group forms hydrogen bonds to both the glycine substrate and to Gly137. (f) Finally, the phenol group of Tyr21, to test a proposal that this group polarizes the S–C bond of SAM, facilitating thereby the S_N2 reaction.

In this model, seven centers had to be frozen (indicated by stars in Fig. 1c). Without these constraints the various groups fly apart and form complexes that do not bear resemblance to the original structure. With constraints, the methyl transfer step could be studied and analyzed. The calculations have confirmed that the methyl transfer step occurs in a single S_N2 step with a calculated barrier of 15.0 kcal/mol and a reaction energy of −14.1 kcal/mol. It is interesting to compare these values to the gas phase results. The barrier without PCM(ε=4) is calculated to 14.3 kcal/mol and the reaction energy to −11.4 kcal/mol. Both these values are quite close to the solvent results, further validating the adequacy of the quantum model. In the same study, the various active site groups were added or eliminated from the model, one at a time. By doing this, it could be shown that hydrogen bonds to the amino group of the substrate lower the reaction barrier, whereas hydrogen bonds to the carboxylate group of the substrate raise the barrier [15].

Another example of this kind of models is a recent study on the catalytic mechanism of limonene epoxide hydrolase (LEH). This enzyme catalyzes the hydrolysis of limonene-1,2-epoxide to give limonene-1,2-diol (Fig. 6a), a reaction that is a part of the limonene degradation pathway.

A recent crystal structure of LEH revealed that the active site consists of a pocket of five charged and polar residues [21]. Based on the structure and also mutagenesis experiments, the following reaction mechanism has been suggested for LEH [21] (Fig. 6b). Asp101 is proposed to donate a proton to the oxirane ring of the substrate and Asp132 abstracts a proton from the lytic water molecule, facilitating nucleophilic attack on the epoxide carbon. Arg99 positions the carboxylate groups of the two aspartates and assists also in charge stabilization. Two amino acids, Tyr53 and Asn55, help positioning the lytic water molecule in a favorable position for epoxide attack.

The quantum chemical model [22] consisted of the five residues mentioned above, together with the substrate and the water molecule. The two aspartates were represented by acetic acids, the tyrosine by phenol, the asparagine by acetamide, and the arginine by N-methyl-guanidine (see Fig. 7). The points of truncation were kept frozen during calculations to preserve the spatial arrangement of the active site residues. The model had a total size of 80 atoms. A picture of the LEH active site model with (1S,2R,4R)-limonene-1,2-epoxide as substrate is shown in Fig. 7a.

With the help of this relatively small model, several aspects of the catalytic mechanism of LEH could be studied. The reaction was shown to occur in one concerted step which involves epoxide protonation by Asp101, nucleophilic attack by water, abstraction of a proton from water by Asp132, and epoxide ring opening. The gas-phase barrier was calculated to be 16.5 kcal/mol and the reaction energy to be −7.5 kcal/mol. Inclusion of PCM solvent (ε=4) reduced the barrier by 1.6 to 14.9 kcal/mol, and the reaction energy by 2.2 to −9.7 kcal/mol.

The model was furthermore sufficient to provide an explanation for the experimentally observed regioselectivity of limonene-1,2-epoxide hydrolysis, where some substrates are attacked on C1 and others on C2 [22]. The isopropenyl group of limonene-1,2-epoxide was shown to play a crucial role, since it restricts the half-chair conformation of limonene-1,2-epoxide to one of two possible helicities. In this conformation, attack on the different epoxide carbons will lead to either a chair-like or a twist-boat TS structure, the latter resulting in a higher barrier [22].

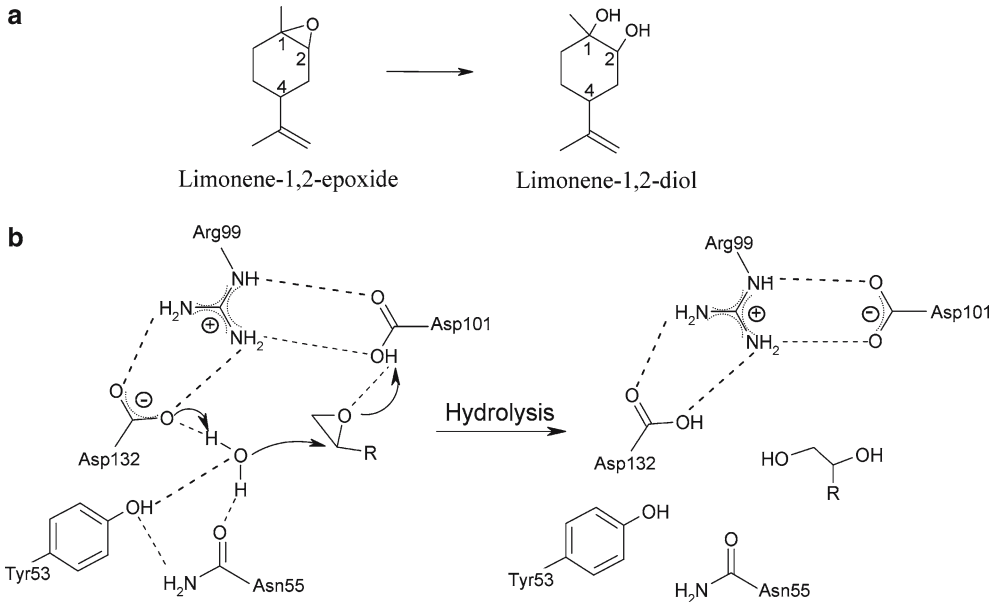

Fig. 6 **a** Reaction catalyzed by limonene epoxide hydrolase (LEH). **b** Proposed mechanism for LEH

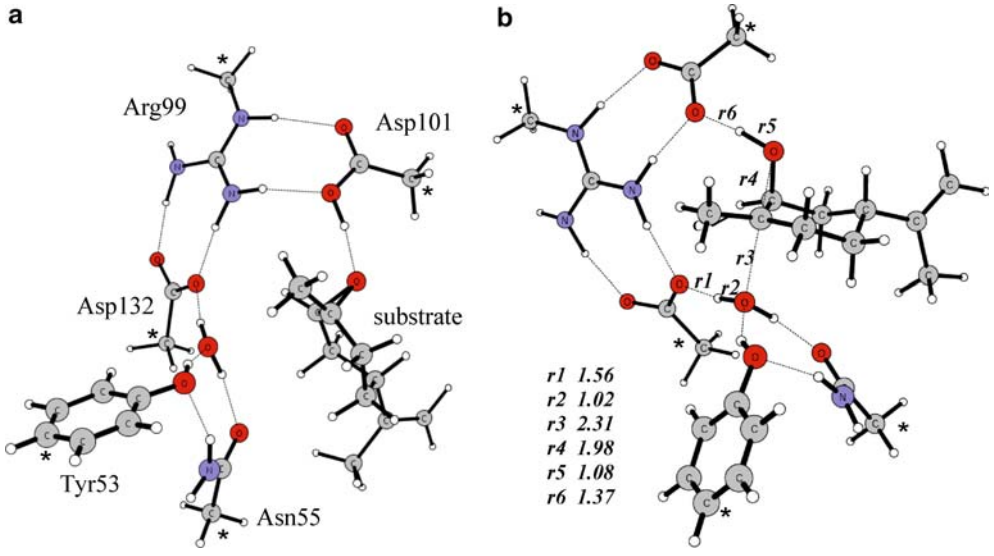

Fig. 7 **a** LEH-active site model including a limonene-1,2-epoxide substrate molecule. **b** Transition state for the hydrolysis at the C1 position of the substrate. Asterisks (*) show atoms kept frozen to their crystallographically observed positions in the calculations

6 Future outlook

We have in this review tried to argue that a relatively small quantum model can actually reproduce the chemistry that takes place in an enzyme active site to a high enough degree that it can be helpful in answering mechanistic questions. How is this field likely to develop in the coming years?

The B3LYP functional has been around for more than a decade. During this period, it has been applied to a wide range of problems, often with great success. We find it unlikely that in the coming few years, some other functional will be developed that by much outperforms B3LYP in terms of the combination of speed and accuracy of reproducing the thermochemistry of such diverse systems.

However, it is quite likely that new methodologies of implementing the B3LYP functional, like efficient code parallelization and linear scaling methods, will make it possible to treat far larger systems than today.

A few years ago, a model consisting of 40 atoms was considered to be large and time consuming. Today, using the same theoretical methods, models consisting of 100 atoms are almost routine. This development can be almost entirely ascribed to the huge advance in computer power. From depending on expensive work stations we have now progressed to

a level where much larger calculations require only ordinary PCs. In particular, parallel calculations on PC clusters have made it possible to perform increasingly larger calculations. Faster and cheaper computers, connected in clusters, will allow for even larger calculations in the coming few years. Active site models will be more and more realistic. As the model size increases, the long-range electrostatic effects will diminish, since most of the solvation is already included quantum mechanically.

However, much larger quantum models will be associated with other shortcomings, such as multiple-minima problems, and sampling will be needed.

Acknowledgements The Wenner-Gren Foundations, the Swedish Research Council, the Carl Trygger Foundation, the Magn. Bergvall Foundation, and the Hagberg Foundation are acknowledged for financial support.

References

1. Becke AD (1988) Phys Rev A38:3098
2. Becke AD (1992) J Chem Phys 96:2155
3. Becke AD (1992) J Chem Phys 97:9173
4. Becke AD (1993) J Chem Phys 98:5648
5. Noodleman L, Lovell T, Han W-G, Li J, Himo F (2004) Chem Rev 104:459
6. Himo F, Siegbahn PEM (2003) Chem Rev 103:2421
7. Siegbahn PEM (2003) Quart Rev Biophys 36:91
8. Siegbahn PEM, Blomberg MRA (2001) J Phys Chem B 105:9375
9. Siegbahn PEM, Blomberg MRA (1999) Ann Rev Phys Chem 50:221
10. Lee C, Yang W, Parr RG (1988) Phys Rev B37:785
11. Vosko SH, Wilk L, Nusair M (1980) Can J Phys 58:1200
12. Guner V, Khuong KS, Leach AG, Lee PS, Bartberger MD, Houk KN (2003) J Phys Chem A 107:11445
13. Curtiss LA, Krishnan R, Redfern PC, Pople JA (1997) J Chem Phys 106:1063
14. Bauschlicher CW Jr (1995) Chem Phys Lett 246:40
15. Velichkova P, Himo F (2005) J Phys Chem B 109:8216
16. Takata Y, Huang Y, Komoto J, Yamada T, Konishi K, Ogawa H, Gomi T, Fujioka M, Takusagawa F (2003) Biochemistry 42:8394
17. Rinaldo-Matthis A, Rampazzo C, Reichard P, Bianchi V, Nordlund P (2002) Nat Struct Biol 9:779
18. Cameron AD, Ridderström M, Olin B, Kavarana MJ, Creighton DJ, Mannervik B (1999) Biochemistry 38:13480
19. Himo F, Siegbahn PEM (2001) J Am Chem Soc 123:10280
20. Feierberg I, Cameron AD, Åqvist J (1999) FEBS lett 453:90
21. Arand M, Hallberg BM, Zou J, Bergfors T, Oesch F, van der Werf M, de Bont JAM, Jones TA, Mowbray SL (2003) EMBO J 22:2583
22. Hopmann KH, Hallberg BM, Himo F (2005) J Am Chem Soc (in press)